

A PS-PULSED E-GUN ADVANCED TO A T-WAVE SOURCE OF MW-LEVEL PEAK POWER

A.V. Smirnov, RadiaBeam Technologies Inc., Santa Monica, CA 90404, USA

Abstract

A coherent source based on an electron gun is considered to deliver high instantaneous power comparable to that available from a few most powerful sources operating at mm-sub-mm wavelengths. A DC or RF E-gun is integrated with a robust, compact, efficient, dismountable radiator inside the vacuum envelope. Resonant Cherenkov radiation is driven by a low-energy photoinjector operated in a custom mode combining strong over-focusing, robust slow-wave structure, and pulse sub-ps photoinjector employing on-cathode beam modulation. Single pulse mode operation is enhanced with filed compression effect at high group velocity. The performance is analyzed analytically and numerically.

INTRODUCTION

A huge variety of applications in biology, medicine, chemistry, solid state physics, radio astronomy, homeland security, environment monitoring, spintronics, advanced spectroscopy, and plasma diagnostics need several orders higher THz peak power than it is available today for universities, middle-sized and small labs and businesses. Many of these applications are related to fast processes, emerging time-domain spectroscopy (TDS), and imaging that require short THz pulses of high intensity.

So far only a few FELs are dedicated to operate at THz frequencies. Typically such an FEL is driven by tens of MeV electron accelerator and contains an undulator and an optical cavity. The first FEL facility to provide THz radiation to users has been the UCSB-FEL (0.3-0.8mm wavelength, ~10kW power in 1-20μs pulse length). The world-largest FEL Facility at JLAB produces a broadband THz radiation [1] with 100W average and about 1MW peak power. To date the Novosibirsk FEL [2] is the most powerful coherent THz source operating at 0.12-0.24mm wavelengths and 0.3% line width to deliver 0.4kW average power and up to ~MW peak power. It comprises 20m long optical cavity, 4m long undulator driven by a 40-50 MeV e-beam accelerated in RF linac with energy recovery. The ENEA-Frascati FEL-CATS source operates in the 0.4-0.7 THz range with about 10% FWHM line width [3] in a super-radiant mode without long optical cavity. A ~1.5 kW power is measured in 5-μs macropulse at 0.4 THz (corresponding to up to 8kW peak in each 3-10 ps micropulse).

More compact, but still powerful, undulator-free, sub-mm wavelength source is considered here. The beam is microbunched on the photocathode with laser using beatwave or multiplexing technique. Important property exploited in the concept is capability of natural focusing of the intense electron beam down to sub-wavelength spot

size in a conventional RF high-brightness photoinjector. These two remarkable features allow effective THz radiation resulted from interaction between high-impedance, slow-wave structure and very high-density, microbunched electron beam.

DESIGN FEATURES

The design concept of the radiator integrated into the E-gun driver is illustrated in Figure 1. The radiator can be based on periodic structure (gratings) or dielectric (PECVD diamond). It may be circular (capillary), rectangular, or planar. The source can operate in two modes: single microbunch and train of microbunches with corresponding laser system.

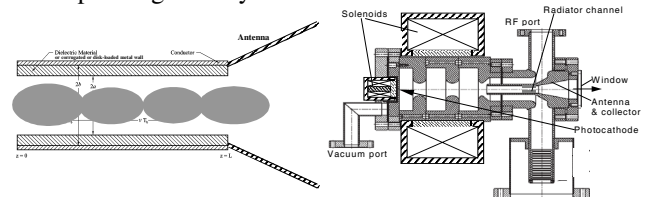


Figure 1: LEFT: THz extractor scheme (radiator). RIGHT: Schematic layout of sub-mm source based on 2-cell, pulse RF or DC-RF electron gun.

Different schemes of THz and exhaust electron beams separation and utilization are exemplified in Figure 2. Simple tapering of the radiator channel turns it into a broader spectrum source for powerful time domain spectroscopy or active “colorful” imaging for inspection and security applications.

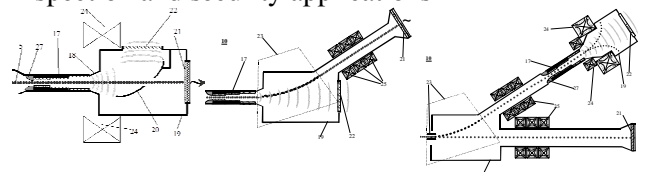


Figure 2: Schematic configurations of a combined T-X-ray source. LEFT: straight electron beam and bended THz beam. MIDDLE: bended electron beam and straight THz beam; RIGHT: alternating electron beam deflected on X-ray target or THz radiator with e-beam scattering and dumping.

A capillary channel has already been used in a number of wakefield research setups (see, e.g., [4]). It is exemplified in Figure 3, left. Radiation directivity can be enhanced with optimized shaping of the dielectric (see Figure 3, right). By sacrificing shunt impedance (see Table 1) one can make the radiator much more robust to sustain THz-field-induced stress and heat as well as beam halo

interception in a narrow channel. Such a non-circular design is shown in Figure 4.

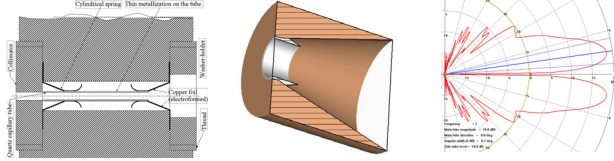


Figure 3: LEFT: Mechanical insertion of a metallized quartz capillary tube into holders (one of them is antenna). The metallization layer is limited by \sim micron to provide minimal mechanical and thermal stability (skin depth $<0.1 \mu\text{m}$ at 1THz). MIDDLE: Shaped dielectric. RIGHT: Radiation diagram with improved directivity.

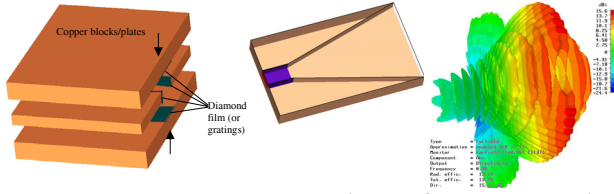


Figure 4: LEFT: Exploded view of a robust, high average power, planar radiator. MIDDLE: a cut-view of planar slot antenna attached to square diamond-coated or grated capillary tube. On the right: 3D diagram of far-field pattern radiated from the square channel.

Table 1. TM_{01} mode parameters for a capillary channel at 0.95-0.97 THz resonant frequency and different coating materials.

Material	ϵ	a, μm	d, μm	R/Q, kOhm/m	β_{gr}	Q/1000
Teflon	2.1	300	31	14.7	0.82	1.9
		520	26	1.07	0.89	2.4
Barium tetra-titanate	37	300	30	27.7	0.127	0.6
Sap-phire	11	300	14	18.9	0.76	1.2
SiO_2	3.8	336	19	12.4	0.83	2.1
Dia-mond	5.7	336	16	12.7	0.82	1.8
		300		8	0.83	1.7

The limits imposed by space charge 3D effects in the Cherenkov THz radiator do not allow utilizing efficiently a sub-ps laser burst carrying more than 50-100 μJ energy. To overcome this limit and produce higher THz energy one can use longer laser pulses of the same energy but modulated intensity. One way to introduce THz premodulation in the long-bunch mode is photomixing. The metal photocathode (usually copper or magnesium) has to be illuminated by a laser (usually Neodymium or Sapphire laser at UV harmonic) having two (or more) lines with \sim THz frequency separation. The beatwave option does not require any interaction space or ballistic drift [5]; it still possesses coherency and possibility of direct synchronization and tuning. This method was proposed for superradiant FEL [6] and Smith-Purcell FEL

[7]. Two (or more) laser lines with a \sim THz frequency shift can be created in different ways. Laser systems for photoinjectors a capable to deliver about 0.3-3mJ (in UV) per 5-20ps pulse using chirped pulse technology with stretcher/compressor. For a typical laser system [8] the required modification is just an addition of one mode locked tunable oscillator to provide a two-line seeding generation with appropriate frequency shift 0.67-1 THz (or 1.2-1.8nm for 744nm before frequency tripling). This frequency range is within the bandwidth of the linear regenerative amplifier (e.g., Ti:Supphire amplifier TSA-50 Positive Light) and the rest of the same laser system can be used.

The THz field induced in the channel is evaluated analytically in time domain in Figure 5 assuming a 0.6mm aperture channel having dielectric coating with $\epsilon=2.1$ and 31 μm thickness and a cosine squared charge distribution resulted from two-wave 0.96THz beating. Neglecting phase space dilution and debunching, detuning and transverse effects it gives bunch formfactor 0.5 and $P=8.2\text{MW}$ peak power at $I=60\text{A}$ beam current. To include the 3D transient beam dynamics effects PIC simulations have been performed.

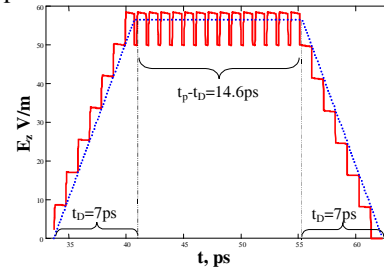


Figure 5: Field amplitude profiles calculated analytically [10] at $z=L$. Accelerated beam pulse length 21.6ps, $L=1\text{cm}$, filling time 40.7ps, drain time 7ps, formfactor=0.5, $r/Q=14.7\text{kOhm/m}$, $Q=1900$, and $\beta_{\text{gr}}=0.82$ at $f=0.96\text{THz}$.

PERFORMANCE SIMULATIONS IN A BEATWAVE MODE

The setup of Figure 1(right) is used for ASTRA simulations. The required focusing is provided by both magnetostatic and RF fields of the injector given in Figure 6.

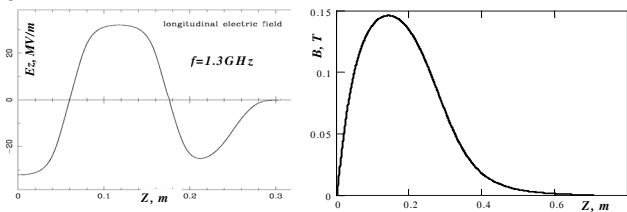


Figure 6: Longitudinal RF electric and magnetostatic field profiles used in simulations of the 2-cell RF photoelectron gun.

The result of optimized beam transport at $I \approx 108\text{A}$ beam current and $E_z=32\text{MV/m}$ cathode field is shown in Figure

7 at laser pulse length is 26 ps, bunch charge is 2nC, maximum RF electric field in the accelerating cavity is $E_{z\max}=32$ MV/m, $B_{z\max}=1.46$ kGs, and beam kinetic energy is 4 MeV. The beam waist rms radius is $110\mu\text{m}$ at $Z=0.326\text{m}$ distance from the cathode. Unusually large laser spot on the cathode ($\sim 3\text{mm}$ vs. sub-mm rms radius) and magnetic field (1.46kG vs. 1kG maximum) resulted from the wavelength limit imposed on the beam waist size.

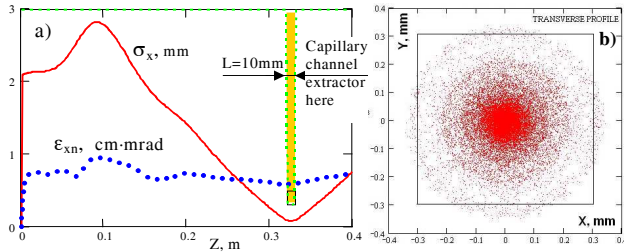


Figure 7. Beam rms horizontal (or vertical) dimension (solid curve) and normalized, transversally uncorrelated emittance (dotted line) plotted as a function of the distance from the cathode (a), and beam transverse profile at the waist (b).

Overall particle losses are 2% and 3.1% for quadratic and circular 1 cm long channels correspondingly for the same $\varnothing 0.6$ mm minimal beam aperture and radial transverse distribution on the cathode. The most of this loss takes place in the channel entrance for the beam head and tail that can be easily collimated, whereas the bulk of the beam (between the two local waists, see Figure 8 and clip [9]) loses less than 1.4% of particles inside the channel. Formfactor optimization and generated field results are shown in Figure 9. In our beatwave model the beam pulse compression during acceleration require $\Delta f=0.657$ THz on-cathode modulation to get the 0.958 THz resonance.

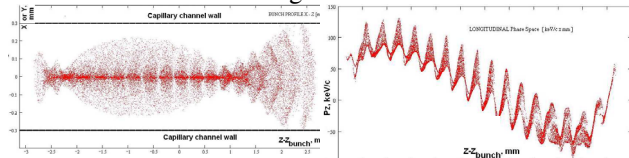


Figure 8: LEFT: Beam X-Z or Y-Z transverse profile inside the capillary channel. Modulation is produced with two-wave beating having 1.55ps period of intensity at the cathode. Laser flat-top pulse length is 26ps, the capillary channel center is positioned at $z=0.326\text{m}$ from the cathode (see animation [9]). RIGHT: Longitudinal phase space of the microbunched beam near its waist in the capillary channel.

The beam-induced fields are calculated as superposition of radiation of each macroparticle (up to $\sim 50,000$ particles) in time domain taking into account high group velocity effects [10] resulted from large gap-to-wavelength ratio and changing formfactor: the microbunch is overfocused and its 3D shape changes rapidly in the interaction space. Peak THz power is 5.7 MW, power averaged over the pulse 1.3 MW, terahertz energy radiated by the 2nC premodulated bunch is 9 μJ .

ISBN 978-3-95450-125-0

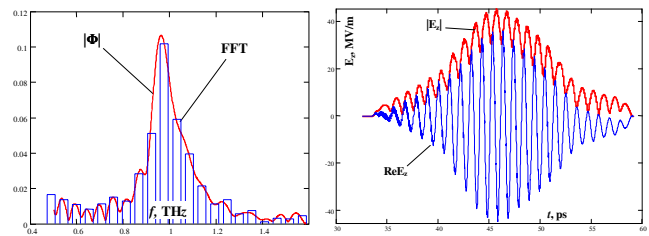


Figure 9: LEFT: Formfactor as a function of frequency at $z=0.326\text{m}$. RIGHT: Output longitudinal electric field amplitude and its real part.

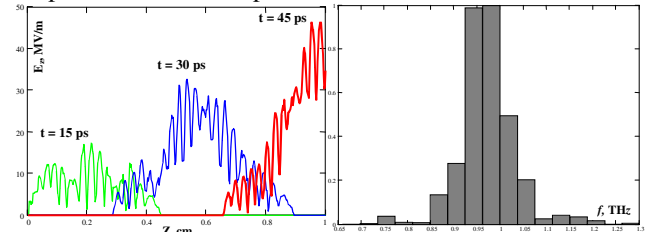


Figure 10: LEFT: Electric field amplitude profile along the capillary channel at different time moments (see animation [11]). RIGHT: Electric field spectrum corresponding to Figure 9.

ACKNOWLEDGMENTS

This work has been supported in part by the Department of Energy (DOE) under the contracts #02-07ER84877 and W21P4Q-12-C-0212. The author is grateful to Pietro Musumeci for experimental confirmation of 3D sub-mm microbunching performed at UCLA PBPL with S-band RF photoinjector.

REFERENCES

- [1] <http://www.usarmythz.com/THz/R+D/THz-HP-Williams.shtml>
- [2] www.kinetics.nsc.ru/center/public/st05.pdf
- [3] Doria A.; Gallerano G.P.; Giovenale E.; Messina G.; Spassovsky I, *Phys. Rev. Lett.* V. 93 (2004) 26481.
- [4] H. Badakov, et al. E-169: Wakefield Acceleration in Dielectric Structures. <http://www.slac.stanford.edu/grp/rd/epac/Proposal/E169.pdf>
- [5] Reiche S.; Joshi C.; Pellegrini C.; Rosenzweig J.B.; Toshitsky S. Ya.; Shvets G., Proceedings of the 27th Free Electron Laser Conference, IEEE: Stanford, CA, 2005; pp 426-428.
- [6] Huang Y. C. Proceedings on Joint Workshop on Laser-Beam Interactions and Laser and Plasma Accelerators, NTU: Taipei, Taiwan, 2005; p 15-23.
- [7] Huang Y.C.; Chang H. L.; Lin Y.Y. Proceedings of the 28th Free Electron Laser Conference, Bessy: Berlin, Germany, 2006; pp 699-701.
- [8] <http://www.hep.anl.gov/pmalhotr/awa-new/links/laser-system.htm>
- [9] <http://www.vimeo.com/637190>
- [10] Smirnov A.V., Nucl. Instrum. and Meth. 2002 NIM A 480 (2-3), 387-397.
- [11] <http://www.vimeo.com/637228>